JACS
JOURNAL OF THE AMERICAN CHEMICAL SOCIETY

COMMUNICATION

pubs.acs.org/JACS

Significantly Enhancing Catalytic Activity of Tetrahexahedral Pt Nanocrystals by Bi Adatom Decoration

Qing-Song Chen,[†,‡] Zhi-You Zhou,[†] Francisco J. Vidal-Iglesias,[‡] José Solla-Gullón,[‡] Juan M. Feliu,[*,‡] and Shi-Gang Sun[*,†]

[†]State Key Laboratory of Physical Chemistry of Solid Surfaces, Department of Chemistry, College of Chemistry and Chemical Engineering, Xiamen University, Xiamen, 361005, China

[‡]Institute of Electrochemistry, University of Alicante, E-03080 Alicante, Spain

Supporting Information

ABSTRACT: Tetrahexahedral Pt nanocrystals (THH Pt NCs) bounded by high-index facets possess a high density of active sites and display therefore a higher catalytic activity in comparison with those enclosed by low-index facets. In the current communication, we report, for the first time, the decoration of THH Pt NC surfaces by using Bi adatoms and have demonstrated that the catalytic activity of the Bi decorated THH Pt NCs toward HCOOH electrooxidation has been drastically enhanced in comparison with bare THH Pt NCs. It has also been revealed that the catalytic activity of Bi decorated THH Pt NCs for all coverages investigated always exhibits a higher catalytic activity that is about double that of Bi decorated Pt nanospheres. The study is of great importance regarding both fundamentals and applications.

Platinum is one of the best single metal catalysts and is used indispensably in chemical industry, petrochemical industry, automobile exhaust purification, and fuel cells, owing to its excellent reactivity and stability.[1] However, the price of Pt is extremely high due to the rare reserve on the earth and the continuing increase in demand. Improving the activity and utilization efficiency of Pt catalysts is therefore the key issue in development of relevant catalysis fields. In a recent investigation, tetrahexahedral Pt nanocrystals (THH Pt NCs) bounded by {730} and vicinal high-index facets have been synthesized by Tian and co-workers.[2] These nanocrystals have high thermal stability even when they were heated to 815 °C and exhibit a high catalytic activity. It has been demonstrated that the catalytic activity of the THH Pt NCs (ca. 81 nm in diameter) is 2−4 times as high as that of commercial Pt/C (3.2 nm) catalysts toward electrooxidation of both formic acid and ethanol. This high catalytic activity has been attributed to the high density of active sites that are composed of low coordination atoms located in steps, kinks, and ledges of the high-index facets.

Besides the effect of surface structure on atomic arrangement, the performance of catalysts is also closely related with their composition due to the mediation of chemical structure. Irreversible adsorption of adatoms (such as Bi, Sb, Te, and As) has been widely applied to modify Pt single crystal electrodes. The effects of Bi to formic acid oxidation on three basal planes and stepped surfaces vicinal to Pt(111) were investigated systematically.[3] It has been demonstrated that formic acid oxidation can be significantly enhanced by Bi (e.g., 40 times for Bi decorated Pt(111)),[3b] and the Bi adatoms' effect of inhibiting poison formation depends on the terrace length and step symmetry.[3d−f] To the best of our knowledge, formic acid oxidation on Bi modified electrodes of Pt single crystal planes lying in the [001] crystallographic zone such as (210), (310), etc. has not been explored so far. A few studies reported Bi decoration on Pt nanoparticles while they are exclusively polycrystalline or those enclosed by low-index facets ({111} or {100}).[4] The {730} and vicinal high-index facets that enclose the THH Pt NCs are composed of subfacets (210) and (310) (see Figure S3 in Supporting Information [SI]). It is therefore of great importance to study the Bi decoration on THH Pt NCs and to boost consequently the catalytic activity of THH Pt NCs. With this aim, Bi irreversible adsorption was introduced to decorate the surface of THH Pt NCs. Significant enhancement of catalytic activity of the THH Pt NCs toward formic acid electrooxidation by Bi adatom decoration has been revealed.

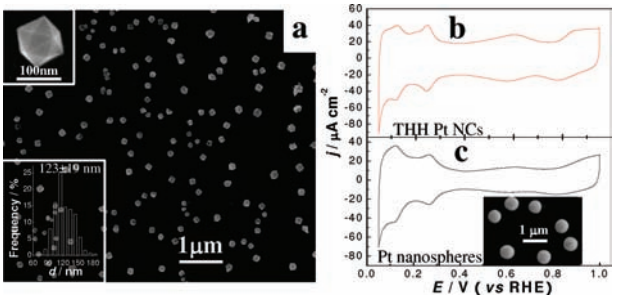

Figure 1. (a) SEM image of THH Pt NCs. The insets are a high-magnification SEM image and size distribution histogram, respectively. (b and c) CVs of THH Pt NCs and Pt nanospheres, in 0.5 M H_2SO_4 solution (scan rate: 50 mV s^{-1}); the inset is SEM image of Pt nanospheres.

The THH Pt NCs at high yield were prepared according to the procedure described elsewhere[2] (see S-2 in SI for details). Figure 1a shows the representative scanning electron microscopy (SEM) image of as-prepared THH Pt NCs. From the high magnification SEM image (inset), it is obvious that the Pt nanocrystal looks like a cube with each face capped by a

Received: May 7, 2011
Published: July 27, 2011

dx.doi.org/10.1021/ja2042029 | J. Am. Chem. Soc. 2011, 133, 12930–12933

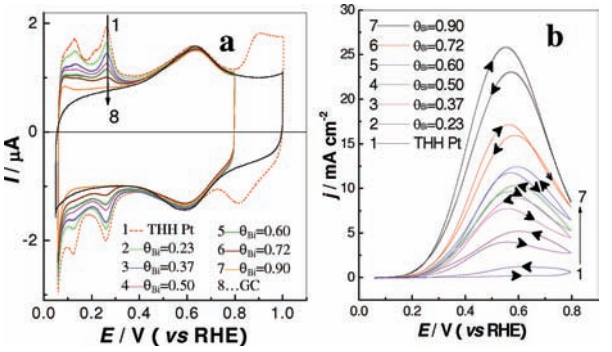

Figure 2. (a) CVs of THH Pt NCs with different Bi coverage as indicated in the figure, in 0.5 M H_2SO_4 solution (scan rate: 50 mV s^{-1}). (b) CVs of THH Pt NCs with different Bi coverage in 0.25 M HCOOH + 0.5 M H_2SO_4 solution (scan rate: 20 mV s^{-1}).

square-based pyramid, indicating a tetrahexahedral shape of Pt nanocrystal. The size distribution histogram of THH Pt NCs gives an average size of about 123 nm which is somewhat bigger than that Tian et al. used ($\bar{d}$ = 81 nm) for formic acid oxidation. This kind of Pt nanocrystals has been verified to be surrounded by {$hk0$} ($h > k$) high-index facets as already described elsewhere.[1d,e,2] As the cyclic voltammograms (CVs) are important fingerprints of Pt surface sites,[5] the surface structure of the THH Pt NCs can be *in situ* characterized by CVs. The active surface area was determined by measuring the charge involved in the hydrogen adsorption region assuming 230 μC cm^{-2} for the total charge after the double layer correction in 0.5 M H_2SO_4 solution.[6] Different features are clearly observed in CVs of THH Pt NCs (Figure 1b) and Pt nanospheres (Figure 1c) that yield a similar CV of a typical polycrystalline Pt electrode.[6] In the hydrogen adsorption/desorption region between 0.06 and 0.6 V, the current peak around 0.12 V corresponds to hydrogen adsorption on (110) sites and that near 0.27 V is associated with hydrogen adsorption on (100) sites.[5] The relative intensity of the hydrogen desorption peak around 0.27 V versus the peak close to 0.12 V ($j_{0.27}/j_{0.12}$) on THH Pt NCs (1.0, Figure 1b) is larger than that on Pt nanospheres (0.7, Figure 1c). Such a value of $j_{0.27}/j_{0.12}$ is representative of CV features of hydrogen desorption on (210) and (310) planes of a platinum single crystal.[1d,5a,5c] As can be seen also in the high potential region, the oxygen adsorption occurs in a clear current peak near 0.89 V on THH Pt NCs, which is typically characteristic of oxygen adsorption on step atoms on high index facets of the THH Pt NCs,[2] while no such current peak is observable on Pt nanospheres.

Bi decoration on THH Pt NCs was carried out in a dilute solution containing 10^{-5} M Bi^{3+} and 0.5 M H_2SO_4 (see S-4 in SI for details). Figure 2a compares the voltammograms of THH Pt NCs with increasing amounts of Bi on the surface. For comparison, the voltammogram of the bare THH Pt NCs and that of a glassy carbon (GC) electrode are also displayed. For Bi decorated THH Pt NCs the upper potential limit was restricted to 0.8 V (vs RHE) to avoid Bi adatom desorption. The Bi coverage can be evaluated by the blockage of hydrogen adsorption charge and is defined as[4a]

$$\theta_{Bi} = 1 - \theta_H = 1 - \frac{Q_H^{Bi}}{Q_H^{unm}} \quad (1)$$

where Q_H^{Bi} is the charge for hydrogen adsorption on the Bi decorated THH Pt NCs, and Q_H^{unm} is the charge for hydrogen adsorption on bare THH Pt NCs. All the hydrogen charges were determined by integrating the voltammetric current between 0.06 and 0.5 V following the subtraction of the contribution from the GC substrate. Obviously, the hydrogen adsorption/desorption current peaks at 0.12 and 0.27 V decrease gradually as Bi coverage increases. It is interesting to remark that the peak around 0.12 V is blocked faster in comparison with that at 0.27 V. As can be seen, the peak at 0.12 V nearly disappears while leaving part of the peak unblocked at 0.27 V as θ_{Bi} = 0.60. This may be interpreted as the negatively charged center at (110) step sites favoring the adsorption of the relative electropositive Bi atom.[7]

Representative CV profiles of formic acid electrooxidation on Bi decorated THH Pt NCs with varying coverage in 0.25 M HCOOH + 0.5 M H_2SO_4 solution are shown in Figure 2b. It is widely accepted that the formic acid oxidation proceeds through a "dual-path" mechanism on platinum, including the active path of direct oxidation to CO_2 through an active intermediate and the poisoning path in which the catalyst is poisoned by intermediate CO_{ad} derived from HCOOH dissociative adsorption.[8] In the case of bare THH Pt NCs, the facets are mostly composed of (100) and (110) sites that are very active for formic acid dissociative adsorption to form CO species,[9] leading to surface poisoning at low potential. As a consequence, the peak current density in the positive-going potential scan (0.21 mA cm^{-2}) is much smaller than that in the negative-going one (1.22 mA cm^{-2}), in which the surface concentration of adsorbed CO is lower due to its oxidation at higher potential. It is evident that the current increases significantly when the THH Pt NCs are modified by Bi adatoms, accompanied by the negative shift of the onset oxidation potential from ca. 0.3 to 0.08 V. The current keeps increasing as the Bi coverage increases until the highest peak current density of 25.8 mA cm^{-2} is achieved at the largest Bi coverage of 0.90. Such a value is 21 times bigger than that obtained on bare THH Pt NCs. It is worthwhile pointing out that in both positive- and negative-going sweeps the oxidation current appears as a maximum in a narrow potential region between 0.55 and 0.61 V depending on the Bi coverage, similar to formic acid oxidation on Bi decorated Pt single crystal electrodes.[3a−c] The CV profiles also undergo qualitative changes with the amount of Bi variation; i.e., at low and medium Bi coverage the currents in the negative-going sweep are bigger than that in the positive-going one, while the positive-going current becomes always larger than the negative-going one when the Bi coverage is above 0.7. This can be ascribed to the absence of poison formation at high Bi coverage (see S-5 in SI).

To better understand the electrocatalytic activity of Bi decorated THH Pt NCs toward formic acid oxidation, chronoamperometric curves were recorded. Figure 3a displays the comparison of current−time transients at 0.3 V on the THH Pt NCs electrode and those on the Bi decorated ones. It can be seen that the currents at a given potential follow the same trend as those observed in Figure 2b; i.e., the oxidation currents increase along with increasing Bi coverage. The current density of formic acid oxidation on THH Pt NCs is very small and quickly decays to nearly zero (0.003 mA cm^{-2}) at 60 s, which is almost negligible with respect to those recorded on Bi decorated ones, e.g. 0.22 and 2.78 mA cm^{-2} on THH Pt NCs with a Bi coverage of 0.23 and 0.90, respectively. This indicates that at low potential the bare THH Pt NCs are easily poisoned by the formic acid dissociative adsorption that yields poisoning CO species, while Bi decoration is helpful to inhibit this reaction. The potential dependence of steady state current densities recorded at 60 s as a

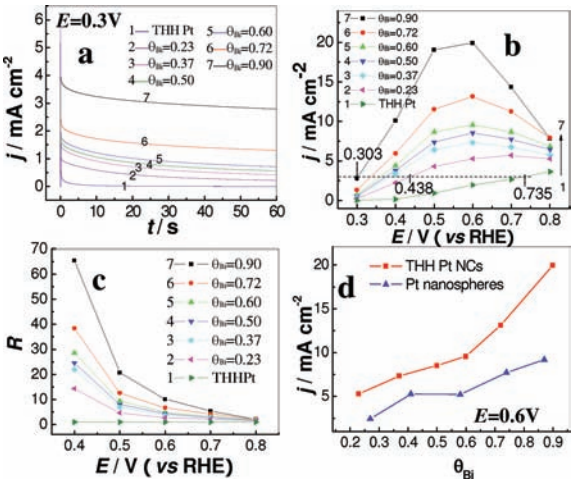

Figure 3. (a) Comparisons of current transients recorded at 0.3 V for formic acid oxidation on Bimodified THH Pt NCs with varying Bi coverage. (b) Comparisons of current densities at 60 s in current time transients of HCOOH oxidation on THH Pt NCs with varying Bi coverage; dash line represents a value of technical interest for fuel cell application of 3 mA cm^{-2}. (c) Potential dependence of the ratio (R) defined as the steady-state current density of Bi decorated THH Pt NCs over that of the unmodified one. (d) Comparison of steady-state current density of formic acid oxidation at 0.6 V on Bi decorated THH Pt NCs with that of Bi decorated Pt nanospheres as a function of Bi coverage. 0.25 M HCOOH + 0.5 M H_2SO_4 solution.

function of Bi coverage is plotted in Figure 3b. The current density recorded at 0.6 V and at 60 s on bare THH Pt NCs is 1.96 mA cm^{-2}. This value is compatible with that reported by Tian et al. about 1.41 mA cm^{-2} measured at a close potential 0.25 V (vs SCE).[2] The current density on Bi decorated THH Pt NCs is always larger than that on an unmodified electrode. For the bare THH Pt NCs, as expected, current densities increase with applied potential, because of the faster electron transfer and lower poisoning at higher potential. However, in the case of Bi decorated THH Pt NCs, the currents increase with increasing potential before 0.6 V, further increasing potential results with the decrease of formic acid oxidation currents, which is more significant for higher Bi coverage electrodes. This phenomenon is in accordance with that observed in the voltammograms shown in Figure 3b.

It is more important to see that at an oxidation current density of technical interest for fuel cell application, as indicated by the dashed line in Figure 3b, the corresponding potential of formic acid oxidation on Bi decorated THH Pt NCs is much lower than that on bare THH Pt NCs. The potential is shifted negatively by about 300 mV even for a small Bi coverage of 0.23 and 432 mV for the largest Bi coverage of 0.90 at the same current density of 3 mA cm^{-2}. As shown in Figure 3c, the enhancement factor R, which is defined as the ratio of the current density measured on Bi decorated THH Pt NCs versus that acquired on bare THH Pt NCs at the same potential, varies in a large range from 65 to 1.5 depending on the electrode potential and Bi coverage. Interestingly, the bigger R values correspond to lower potentials due to the suppression of CO formation, which is of great importance in the case of practical application in fuel cells, because a higher power density can be outputted by a fuel cell with an anode that could work at lower potentials, and also the anode working at low potential favors the stabilization of Bi adatoms, resulting in a prolonged life of the catalyst. For comparison, formic acid oxidation on Bi decorated Pt nanospheres has also been carried out under the same procedures used for THH Pt NCs. As shown in S-6 in SI, the catalytic activity of Pt nanospheres for formic acid oxidation is also enhanced by Bi decoration and follows the similar trend with variation of Bi coverage as that observed with THH Pt NCs. It is interesting to see that the steady-state current densities measured from the current−time transients recorded on Bi decorated THH Pt NCs are always bigger than those on Bi decorated Pt nanospheres. A comparison is illustrated in Figure 3d with the oxidation potential at 0.6 V. The current densities on THH Pt NCs are almost double those on Pt nanospheres for all Bi coverages investigated. This result further confirms that Bi decoration can significantly boost the catalytic activity of THH Pt NCs, on which the surface is of ($hk0$) structure together with active sites at the corners and edges of the nanocrystals.

The above results from both cyclic voltammetry and chronoamperometry demonstrated that the catalytic activity of THH Pt NCs toward formic acid oxidation, which is superior to that of Pt nanospheres and commercial Pt/C catalysts, can be further significantly enhanced through Bi decoration. The mechanism of Bi effects may be explained as follows. From the knowledge of formic acid oxidation on Pt single crystals, the dehydration path to form CO requires an ensemble of surface sites,[10] while the adsorbed Bi diminishes the number of available ensembles and greatly suppresses the poison formation (third body effect). Moreover, the preferential decoration of Bi on the low coordination (110) sites, which are the most active for formic acid dissociative adsorption,[9] also results in decreasing the CO formation rate. In contrast, the direct oxidation of formic acid through an active intermediate only needs an isolated Pt site, since no coadsorption of OH is required for the oxidation.[11] Incidentally, larger currents for formic acid oxidation, even with very small Bi coverage, indicate that Bi adatoms may also contribute to the enhancement via an electronic effect.[12] This effect has been simulated by a simple model in which the electronic effect is limited to the platinum nearest neighbors.[10a]

In summary, the catalytic activity of THH Pt NCs toward formic oxidation has been significantly improved through Bi decoration, in which Bi adatoms yield a third body effect and may also contribute an electronic effect. It has been also revealed that the catalytic activity of the Bi decorated THH Pt NCs is superior to that of Bi decorated Pt polycrystalline nanospheres. The present study has shed new light on further boosting the catalytic activity of high-index faceted Pt nanocrystals.

■ ASSOCIATED CONTENT

Supporting Information. Experimental details and additional data. This material is available free of charge via the Internet at http://pubs.acs.org.

■ AUTHOR INFORMATION

Corresponding Author
sgsun@xmu.edu.cn; juan.feliu@ua.es

■ ACKNOWLEDGMENT

This work has been financially supported by the Natural Science Foundation of China (Grant Nos. 20833005 and 21021002) and Ministerio de Educación y Ciencia of Spain

(Feder) through Project CTQ2006-04071/BQU. Q.S.C. also acknowledges the fellowship support of the China Scholarship Council.

REFERENCES

(1) (a) Zaera, F. *Appl. Catal., A* **2002**, *229*, 75. (b) Heck, R. M.; Farrauto, R. J. *Appl. Catal., A* **2001**, *221*, 443. (c) Chen, A. C.; Holt-Hindle, P. *Chem. Rev.* **2010**, *110*, 3767. (d) Tian, N.; Zhou, Z. Y.; Sun, S. G. *J. Phys. Chem. C* **2008**, *112*, 19801. (e) Zhou, Z. Y.; Tian, N.; Huang, Z. Z.; Chen, D. J.; Sun, S. G. *Faraday Discuss.* **2008**, *140*, 81.

(2) Tian, N.; Zhou, Z. Y.; Sun, S. G.; Ding, Y.; Wang, Z. L. *Science* **2007**, *316*, 732.

(3) (a) Clavilier, J.; Femandez-Vega, A.; Feliu, J. M.; Aldaz, A. *J. Electroanal. Chem.* **1989**, *261*, 113. (b) Clavilier, J.; Fernandez-Vega, A.; Feliu, J. M.; Aldaz, A. *J. Electroanal. Chem.* **1989**, *258*, 89. (c) Lopez-Cudero, A.; Vidal-Iglesias, F. J.; Solla-Gullon, J.; Herrero, E.; Aldaz, A.; Feliu, J. M. *J. Electroanal. Chem.* **2009**, *637*, 63. (d) Macia, M. D.; Herrero, E.; Feliu, J. M. *Electrochim. Acta* **2002**, *47*, 3653. (e) Macia, M. D.; Herrero, E.; Feliu, J. M.; Aldaz, A. *Electrochem. Commun.* **1999**, *1*, 87. (f) Macia, M. D.; Herrero, E.; Feliu, J. M.; Aldaz, A. *J. Electroanal. Chem.* **2001**, *500*, 498. (g) Smith, S. P. E.; Ben-Dor, K. F.; Abruna, H. D. *Langmuir* **2000**, *16*, 787.

(4) (a) Lopez-Cudero, A.; Vidal-Iglesias, F. J.; Solla-Gullon, J.; Herrero, E.; Aldaz, A.; Feliu, J. M. *Phys. Chem. Chem. Phys.* **2009**, *11*, 416. (b) Jung, C.; Zhang, T.; Kim, B. J.; Kim, J.; Rhee, C. K.; Lim, T. H. *Bull. Korean Chem. Soc.* **2010**, *31*, 1543.

(5) (a) Clavilier, J.; Armand, D.; Sun, S. G.; Petit, M. *J. Electroanal. Chem.* **1986**, *205*, 267. (b) Clavilier, J.; El Achi, K.; Rodes, A. *Chem. Phys.* **1990**, *141*, 1. (c) Furuya, N.; Shibata, M. *J. Electroanal. Chem.* **1999**, *467*, 85.

(6) Chen, Q. S.; Solla-Gullón, J.; Sun, S. G.; Feliu, J. M. *Electrochim. Acta* **2010**, *55*, 7982.

(7) (a) Chen, Q. S.; Berna, A.; Climent, V.; Sun, S. G.; Feliu, J. M. *Phys. Chem. Chem. Phys.* **2010**, *12*, 11407. (b) Herrero, E.; Climent, V.; Feliu, J. M. *Electrochem. Commun.* **2000**, *2*, 636.

(8) (a) Capon, A.; Parsons, R. *J. Electroanal. Chem.* **1973**, *45*, 205. (b) Sun, S. G.; Clavilier, J.; Bewick, A. *J. Electroanal. Chem.* **1988**, *240*, 147. (c) Chen, Y. X.; Heinen, M.; Jusys, Z.; Behm, R. J. *Langmuir* **2006**, *22*, 10399.

(9) Sun, S. G.; Lin, Y.; Li, N. H.; Mu, J. Q. *J. Electroanal. Chem.* **1994**, *370*, 273.

(10) (a) Leiva, E.; Iwasita, T.; Herrero, E.; Feliu, J. M. *Langmuir* **1997**, *13*, 6287. (b) Neurock, M.; Janik, M.; Wieckowski, A. *Faraday Discuss.* **2008**, *140*, 363. (c) Cuesta, A.; Escudero, M.; Lanova, B.; Baltruschat, H. *Langmuir* **2009**, *25*, 6500.

(11) Lipkowski, J.; Ross, P. N. *Electrocatalysis*; Wiley-VCH: New York, 1998.

(12) (a) Herrero, E.; Fernández-Vega, A.; Feliu, J. M.; Aldaz, A. *J. Electroanal. Chem.* **1993**, *350*, 73. (b) Kim, J.; Rhee, C. K. *Electrochem. Commun.* **2010**, *12*, 1731.